

# AD-A275 164

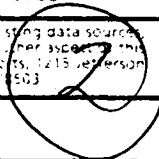


PAGE

Form Approved  
OMB No. 0704-0188

Public report  
publishing and  
collection of  
DTIC High Alt

For response, including the time for reviewing instructions, searching existing data sources, gathering additional information, sending comments regarding this burden estimate or any other aspect of this collection of information, including suggestions for reducing the burden, send them to Washington Headquarters Services, Directorate for Information Operations and Reports, 1215 Jefferson Davis Highway, Suite 1204, Arlington, VA 22202-4302, and Budget Paperwork Reduction Project (0704-0188), Washington, DC 20503



1. AGENCY USE ONLY (leave blank)		2. REPORT DATE December 28, 1993		3. REPORT TYPE AND DATES COVERED Reprint	
4. TITLE AND SUBTITLE Improved Viscous Brake Design Using Simulation				5. FUNDING NUMBERS PR 9261 TA EJ WU 88	
6. AUTHOR(S) George Y. Jumper, Thomas B. Joslyn, Geoffrey R. Kirpa, Alan B. Mironer*					
7. PERFORMING ORGANIZATION NAME(S) AND ADDRESS(ES) Phillips Lab/SXA 29 Randolph Road Hanscom AFB, MA 01731-3010				8. PERFORMING ORGANIZATION REPORT NUMBER  PL-TR-93-2262	
9. SPONSORING / MONITORING AGENCY NAME(S) AND ADDRESS(ES)  <b>DTIC ELECTE</b> <b>JAN 18 1994</b> <b>S A</b>				10. SPONSORING / MONITORING AGENCY REPORT NUMBER	

11. SUPPLEMENTARY NOTES \*SIE, Inc., Lexington, MA  
 Reprinted from Proceedings of the 1993 Summer Computer Simulation Conference  
 Lafayette Hotel, Boston, MA July 19-21 1993 pp 1028-1032

12. DISTRIBUTION STATEMENT (if applicable)  
 Approved for public release; Distribution unlimited

13. ABSTRACT (Maximum length)  
 The SDIO High Altitude Balloon Experiment (HABE) required a rapid controlled descent of a large, heavy payload from a balloon platform. An existing viscous brake concept was chosen for the job, but the short time and space available coupled to the heavy payload resulted in very high power densities. Existing rules of thumb for viscous brakes were insufficient for the design. Viscous brake phenomenology and the particular physical constraints were coded into a modern continuous simulation applications package. After investigating both full dynamic and quasi-steady models, it was decided that the latter was adequate for all but the first and last small fraction of the descent. The model includes temperature dependent viscosity and a heat transfer model. The model been used extensively to investigate the design space and to develop test plans.

**94 1 14 062**

14. SUBJECT TERMS Simulation, Viscous Brake, Thermal Mechanical Model, Viscous Brake Design			15. NUMBER OF PAGES 5
			16. PRICE CODE
17. SECURITY CLASSIFICATION OF REPORT UNCLASSIFIED	18. SECURITY CLASSIFICATION OF THIS PAGE UNCLASSIFIED	19. SECURITY CLASSIFICATION OF ABSTRACT UNCLASSIFIED	20. LIMITATION OF ABSTRACT SAR

IMPROVED VISCOUS BRAKE DESIGN USING SIMULATION

George Y. Jumper, Senior. Aerospace Engineer  
 Thomas B. Joslyn, Aerospace Engineer  
 Geoffrey R. Kirpa, Mechanical Engineer  
 Phillips Laboratory, 29 Randolph Rd  
 Hanscom AFB, MA 01731-3010  
 and  
 Alan B. Mironer, SIE, Inc., Lexington, MA

**ABSTRACT**

The SD10 High Altitude Balloon Experiment (HABE) required a rapid controlled descent of a large, heavy payload from a balloon platform. An existing viscous brake concept was chosen for the job, but the short time and space available coupled to the heavy payload resulted in very high power densities. Existing rules of thumb for viscous brakes were insufficient for the design. Viscous brake phenomenology and the particular physical constraints were coded into a modern continuous simulation applications package. After investigating both full dynamic and quasi-steady models, it was decided that the latter was adequate for all but the first and last small fraction of the descent. The model includes temperature dependent viscosity and a heat transfer model. The model been used extensively to investigate the design space and to develop test plans.

**BACKGROUND**

A unique ascent procedure has been proposed for the HABE experiment. At liftoff, all of the helium will be contained in a "tow balloon". At a designated altitude, the payload will be dropped approximately 500 feet below the tow balloon, allowing the deployment of the main balloon and parachute which are attached to the tow and stored at the top of the payload section. See Figure 1 for a representation of the reel down sequence.

The design of the system is constrained by the following: full reel down must be accomplished within 3.5 minutes to insure that the main balloon is fully deployed before gas begins to flow from the tow balloon to the main balloon; at the end of the 500ft reel down, separation velocity must be low enough to avoid excessive stress on the main balloon and parachute which must provide the final braking force; the fluid temperature must not exceed 450°F to avoid thermal breakdown. A desired capability is that the system should stay within these constraints for initial conditions within the range from 0°F to 100°F.

The Aerospace Engineering Division of the Phillips Laboratory has had extensive experience using reel down systems with integrated viscous brakes (Wagner and Doherty 1958). The requirements for the HABE mission are much more severe in payload weight and time available for the deployment. This causes very high brake power loads, resulting in significant heating of the brake fluid which, in turn, substantially lowers fluid viscosity. If the brake fluid viscosity is too low, thermal runaway could result. If it is too high, reel down will take too long. A mathematical simulation of the deployment was required to assist in the design and test of the reel down system.

**THEORY**

The motion of the system is determined by applying Newton's 2nd Law to each point mass:

$$m \frac{d^2R}{dt^2} = \sum F_i \quad (1)$$

Where:  $m$  = mass  
 $R$  = position vector to center of mass  
 $F_i$  = the  $i^{th}$  force vector

Since reel down would occur at some time after liftoff, it is assumed that the system would be traveling horizontally at the speed of the wind, and that any horizontal relative motion between balloon and payload would be damped out. This reduces the scope of the analysis to the vertical coordinate only.

A free body diagram of each mass is shown in Figure 2. The equation of motion for each mass is:

$$m_1 \frac{d^2y_1}{dt^2} = B - D_y - T - (N_1 + \Delta W) \quad (2)$$

$$m_2 \frac{d^2y_2}{dt^2} = T - (N_2 - \Delta W) \quad (3)$$

Where:  $T$  = Tension in the connection  
 $W$  = Weight  
 $B$  = Buoyancy  
 $D$  = Drag

Subscripts:  
 1 = Balloon and Helium  
 2 = Payload

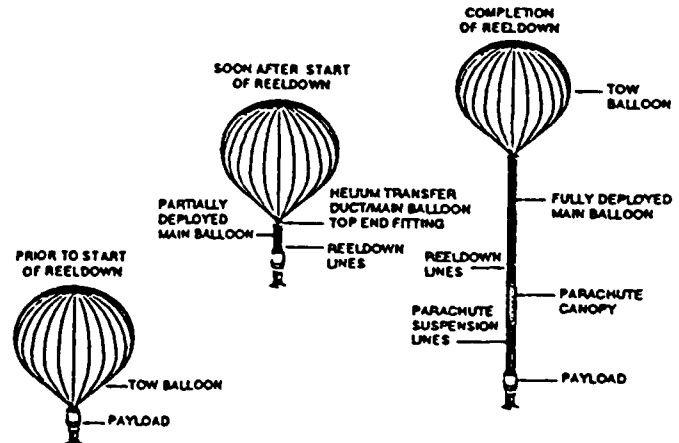


Figure 1. The reel down sequence.

94-01686



and where  $\Delta W$  the weight of the main balloon and parachute that has been extracted from the payload section. This added weight on the upper mass should include the additional force required to accelerate the main balloon and parachute from the velocity of the payload to the velocity of the upper mass. This tension is equal to the instantaneous rate of change of momentum of those items which is negligible for this problem.

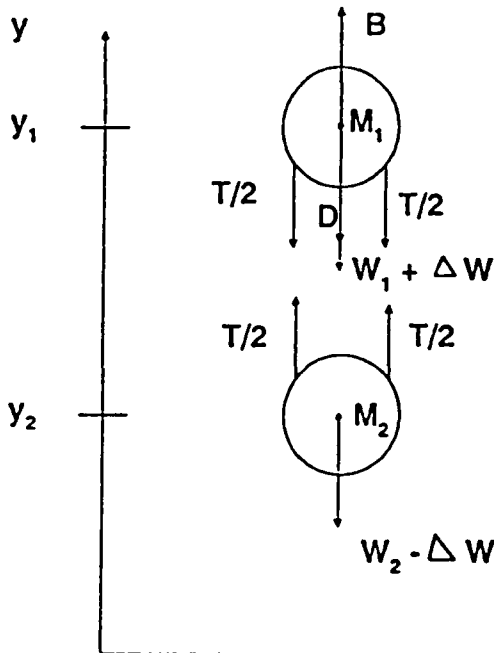


Figure 2. Free Body Diagram of balloon and payload.

Similarly, it is assumed that the combined tension in the cables,  $T$ , is equal at both ends which implies that the cable mass is negligible. The separation or reel down speed is controlled by the tension in the line, which, in turn, is controlled by the viscous brake. The brake is on the shaft connecting the two reels as shown in Figure 3. When Newton's Second Law is applied to a system rotating about a fixed axis the result is:

$$J \frac{d^2\theta}{dt^2} = TR - M_{brake} \quad (4)$$

Where:  $J$  = moment of inertia of the rotating system (slug ft<sup>2</sup>)  
 $\theta$  = angle of rotation (rad)  
 $R$  = radius to cable on reel (ft)  
 $M_{brake}$  = moment caused by brake (lb ft)

The brake moment (Wagner and Doherty 1958) is:

$$M_{brake} = n \pi \nu \rho \omega (r_o^4 - r_i^4) / d \quad (5)$$

Where:  $\nu$  = kinetic viscosity (ft<sup>2</sup>/s)  
 $\rho$  = brake fluid density (slugs/ft<sup>3</sup>)  
 $\omega$  = angular velocity, same as  $d\theta/dt$  (rad/s)  
 $n$  = number of rotors in the brake  
 $r$  = outer or inner radius of active brake surface (ft)  
 $d$  = distance between disk rotors and stators (ft)

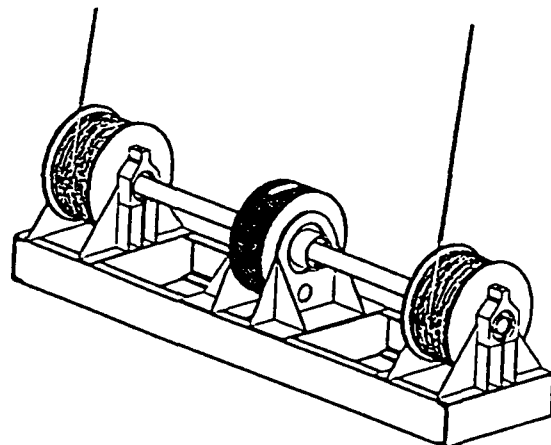


Figure 3. Isometric of brake and reels.

As stated earlier, the HABE brake will be absorbing a lot of power, which will cause fluid heating. The temperature dependence of viscosity for many liquids is known to follow the following relationship:

$$\nu = \lambda \nu_n \exp(B/T) \quad (6)$$

Where  $\nu_n$  is the nominal viscosity for the fluid and  $A$  and  $B$  are constants for the material. For the GE VISCASIL<sup>®</sup> fluids used in the HABE brakes, the constants were found to be 0.003 and 1740 respectively (when  $T$  is measured in K).

The reel down is accomplished by spooling DuPont KEVLAR<sup>®</sup> cable from two straight sided spools. Assuming a continuous reduction of radius with length, the instantaneous radius is:

$$R = \sqrt{R_o^2 - (R_o^2 - R_i^2)l/L} \quad (7)$$

where:  $l$  is the instantaneous length  
 $L$  is the total length

and subscript  $o$  refers to the outer extent of the cable radius when fully wound on the spool, and  $i$  is the radius when fully deployed.

The rate of change of length of cable is related to the turning of the cable by the rotational formula:

$$\frac{dl}{dt} = R \frac{d\theta}{dt} \quad (8)$$

If the cable is assumed to be have infinite stiffness, then the separation of the two masses is exactly determined by the amount of reel down, which reduces the degrees of freedom of the problem to 2. This seems especially justified since DuPont KEVLAR<sup>®</sup> is a very stiff material. With infinite stiffness, the length rolled off the spool,  $l$ , is directly related to the distance between the two masses by the equation:

Dist	Availability
	Statement
A-1 20	

$$l = y_1 - y_2 \quad (9)$$

The approach used to solve the differential equation set was to first solve Equation 4 for the tension,  $T$ , and substitute the result into the two linear equations of motion, Equations 2 and 3. Next, Equations 8 and 9 are used to relate the angular acceleration to the two linear accelerations as follows: Take the second time derivative of Equation 9 to obtain:

$$\frac{d^2 l}{dt^2} = \frac{d^2 y_1}{dt^2} - \frac{d^2 y_2}{dt^2} \quad (10)$$

The time derivative of Equation 8 is:

$$\frac{d^2 l}{dt^2} = \frac{dR}{dt} \frac{d\theta}{dt} + R \frac{d^2 \theta}{dt^2} \quad (11)$$

Combining Equations 10 and 11, and solving for the angular acceleration term, we have:

$$R \frac{d^2 \theta}{dt^2} = \frac{d^2 y_1}{dt^2} - \frac{d^2 y_2}{dt^2} - \frac{dR}{dt} \frac{d\theta}{dt} \quad (12)$$

Equation 12 is then used to remove angular acceleration from the linear motion equations to obtain Equations 13 and 14:

$$\left(m_1 + \frac{J}{R^2}\right) \frac{dV_1}{dt} - \frac{J}{R^2} \frac{dV_2}{dt} = B - M_1 - \Delta N \quad (13)$$

$$- \frac{J(R_0^2 - R_i^2)}{2LR} \left(\frac{d\theta}{dt}\right)^2 - \frac{M_{brake}}{R} - D$$

$$\left(m_2 + \frac{J}{R^2}\right) \frac{dV_2}{dt} - \frac{J}{R^2} \frac{dV_1}{dt} = -M_2 + \Delta N \quad (14)$$

$$+ \frac{J(R_0^2 - R_i^2)}{2LR} \left(\frac{d\theta}{dt}\right)^2 + \frac{M_{brake}}{R}$$

The differential equation solution software, ACSL<sup>®</sup>, can not solve these equations as written, since both linear accelerations appear in each equation. This is easily remedied by using algebraic methods to obtain an equation for either the time derivative of  $V_1$  or  $V_2$ . Only one of them must be isolated for ACSL to solve the problem.

A constant temperature solution of the equations revealed that the system very rapidly converges to the steady state solution of the angular velocity equation, Equation 4. The time to get to this steady state solution is less than one second out of a complete run of almost 200 seconds, as shown in Figure 4. This is fortunate since the steady state solution requires much less computation, and is much easier to use in studying the effects of temperature and other variables.

#### Steady State Solution:

The steady state solution of Equation 4 is obtained by setting the second derivative of  $\theta$  to zero, which yields the static result that the sum of the moments is zero. That is, the torque from the reel down cables is exactly balanced by the torque from the brake. After solving for angular velocity, we obtain:

$$\omega = \frac{TRd}{n\pi v\rho(r_0^4 - r_i^4)} \quad (15)$$

Similarly, the steady state assumption is applied to the equation of motion for the bottom mass (Equation 3) to yield the result that the tension is equal to the weight of the payload minus the amount of balloon and payload that has been deployed. Note that this steady state solution does not result in a constant velocity. As the cable pays out,  $T$  and  $R$  decrease, which tends to decrease the angular velocity. The increasing temperature lowers viscosity which tends to increase angular velocity. The solution is "steady" in that the changes are slow enough that the acceleration terms are not a significant part of the equations for most of the time period of interest.

To complete the description of the steady state solution set, the initial conditions completely determine the right hand side of Equation 15. As  $\omega$  (i.e.,  $d\theta/dt$ ) is determined, Equation 8 is integrated to determine the amount of cable that has been reeled out so that the instantaneous value of  $T$  and  $R$  can be determined. The instantaneous brake power for rotating equipment is the torque times the angular velocity:

$$P_{brake} = T\omega \quad (16)$$

This dissipated power appears as heat in the brake fluid. As the fluid heats up, it transfers heat to the rotors and stators which, in turn, pass it on to the housing and the shaft. The heating period is so short that not very much is transferred to the surrounding air. The heating of the brake was investigated by, first, formulating a detailed thermal model of the brake, then using the results of that model to guide in the formulation of a simpler model for incorporation in the ACSL solution. That model was a three node model which consisted of three equations of the form:

$$M_i C_i \frac{dT_i}{dt} = \left( \sum_j K_{ij} (T_j - T_i) \right) + Q_i \quad (17)$$

Where:  $T_i$  = temperature of the  $i^{\text{th}}$  node  
 $K_{ij}$  = thermal conductance from  $i^{\text{th}}$  to  $j^{\text{th}}$  node  
 $Q_i$  = internal heat generation for the  $i^{\text{th}}$  node  
 $M_i$  = mass of the  $i^{\text{th}}$  node  
 $C_i$  = heat capacity of the  $i^{\text{th}}$  node

The nodes represent the following: 1, the fluid, which was the only node to have any internal heat generation, 2, the rotors and stators, and 3 the housing and shaft. The values used for thermal mass ( $M_i C_i$ ) were 3,990J/K for 1, 21,100J/K for 2, and 14,600J/K for 3 (Mironer 1992). The conductance between 1 and 2 was 680W/K, between 1 and 3 was 47.5W/K, and between 2 and 3 was 9.50W/K. The internal heat generation is the power dissipation computed in Equation 15.

#### INITIAL DESIGN CALCULATIONS

The steady state program was run with various nominal fluid viscosities to determine what was required for acceptable operation of the system. With an initial temperature of 60°F, and a nominal viscosity of 125,000 centistokes, the 500 foot line deployed in 200 seconds. With both the payload weight and the radius of the line on the reel decreasing with time, the torque on the brake is monotonically decreasing with time as shown in

Figure 5. If viscosity were constant, brake reel speed would also decrease, but, in fact, the reel speed increases as shown in Figure 6. The reason for this is that the power dissipation into the brake (Figure 7) is increasing the temperature of the brake fluid (Figure 8), which is decreasing the viscosity. The problem is fully coupled in that the increasing rollout velocity increases the power, further increasing the heating, which further reduces viscosity.

While the above description suggests a potential run-away situation, the final result is fairly benign with the proper brake fluid viscosity. The decreasing torque finally balances the effect of increasing temperature to slow down the rotational speed. The decreasing radius also results in decreasing rollout velocity as shown in Figure 9. This particular case is judged successful since brake fluid temperature, total time, and final rollout velocity were within the design constraints. This viscosity will behave differently at different starting temperatures, as shown in Figure 10.

#### PROTOTYPE TESTING

At this point it is proper to point out that the model described above, while sophisticated for standard brake design practice, contains many assumptions and simplifications which lead to inaccuracies in the final results. Some of the major uncertainties are the small differences in geometry from one rotor-stator working surface to the next due to manufacturing tolerances, the actual viscosity of the fluid at the shear rates of the test, the accuracy of a single average temperature in determining the correct average viscosity of the fluid in the brake, the accuracy of the 3 node model for predicting the heat transfer events of the brake, and the accuracy of the thermal masses and the thermal conductances in the model. A horizontal brake reel roll out test was planned to insure that the system and components performed satisfactorily under loads expected for the operational system and to validate the system model. Only by this development testing could we have confidence of success when the system is dropped from a balloon.

Two trucks were used to perform the horizontal brake reel test. One truck was used to hold the system in place and another truck pulled out the Kevlar Line. Since the trucks were available for only a limited amount of time, and since each test will require at least 2 hours for cool down of the brake and rewinding of the line on the spools, the probable number of tests is from 2 to 4. In order to design the test for maximum useful data, several possible test runs were simulated with the system model. Accurate speedometer and load cell readout was available in the truck cab.

The basic model was modified to simulate constant applied force, constant pull out speed, and constant applied power. The constant force resulted in a speed curve which was similar to the expected operational performance shown in Figure 9. The resulting power input was proportional to the speed curve. Constant speed operation resulted in high initial force which decreased to a shallow minimum near the midpoint of the pull, then increased dramatically near the end of the run. The constant power runs resulted in an increasing, then decreasing speed requirement and a decreasing, then increasing force input.

The best option for calibration of the thermal

model was the constant power run. It resulted in the longest period of nearly linear temperature rise, but this condition imposes the requirement of either maintaining a variable speed or a variable pulling force, which would probably be difficult for the driver to accomplish. For this reason, this option is not recommended for the test.

The constant speed tests had the advantage of a considerable long period of nearly constant load, followed by a gradually increasing load toward the end of the run. This allowed a thorough mechanical test of the system at nearly nominal loads followed by a final increase to proof test load. This condition also results in a nearly linear temperature increase over a long part of the experiment, which would facilitate calibration of the thermal model. The disadvantage of this test option is that the chosen speed must be low enough to avoid damaging loads at the start and end of the run which keeps average power and total energy levels lower than that expected on the HABE deployment drops, which results in small increases in brake fluid temperature.

The constant pull force option has the advantage that the average power and total energy levels can be of the same magnitude as the actual HABE deployments. This gets the fluid temperature up to expected operational levels, thereby validating the brake torque model throughout the operational envelope.

It is assumed that the driver will have large readout gages for both force and speed in the low range of interest. While the driver's ability to maintain either a constant speed (with varying pull force) or a constant pull force (with varying speed) is not assured, so long as the actual speed and force data are known, the model can be calibrated.

#### CONCLUSION

The continuous simulation software proved invaluable in both the design and testing of the new brake assembly. In fact, without a simulation model it might have been impossible to arrive at a satisfactory design for the brake, or even be able to interpret the test data.

#### ACKNOWLEDGEMENTS

This work was supported by the Department of Defense, Strategic Defense Initiative Office. The authors also wish to thank the other members of the Air Force mechanical design team, George McPhetres and Tim Cooper, illustrator M.J. Flanagan (SIE, Inc.), and the design and fabrication team at Wentworth Institute of Technology.

#### REFERENCES

Wagner, W.C. and F. X. Doherty 1958, "Device for Lowering Loads from High-Altitude Balloons", AFCRC-TR-240, Air Force Cambridge Research Center, Bedford, Massachusetts, July 1958.

Mironer, Alan, "Thermal Analysis of BABE Brake", SIETM: 92-04, SIE, Inc., Lexington, Massachusetts, 20 October, 1992.

#### BIOGRAPHY

George Jumper received his PhD in Mechanical Engineering in 1975 from the Air Force Institute of Technology, Wright Patterson AFB, OH. He taught at the United States Military Academy and Worcester Polytechnic Institute. In his current position, he performs engineering analysis of satellites, rockets, balloons, and payloads. His research interests include the simulation of atmospheric and space vehicle trajectories, and thermal, mechanical and biological systems.

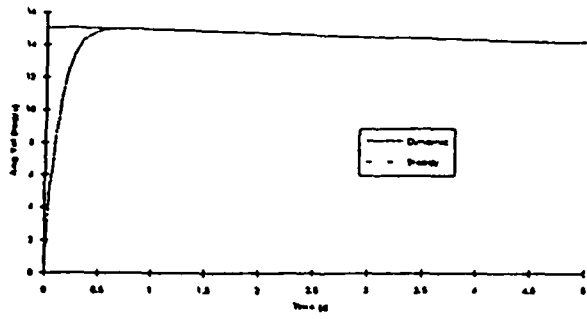


Figure 4. Comparison of dynamic to steady state solution for a constant temperature

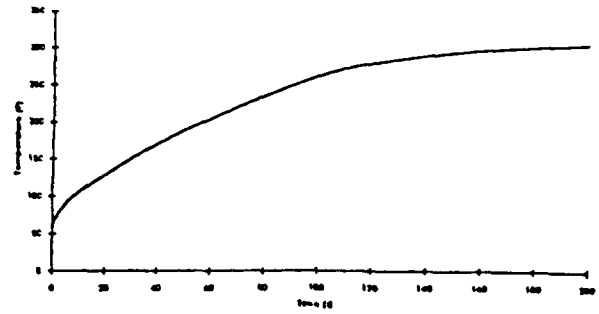


Figure 8. Brake fluid temperature during rollout.

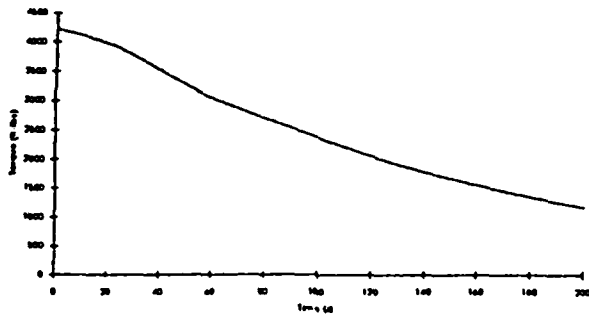


Figure 5. Brake torque during reeldown.

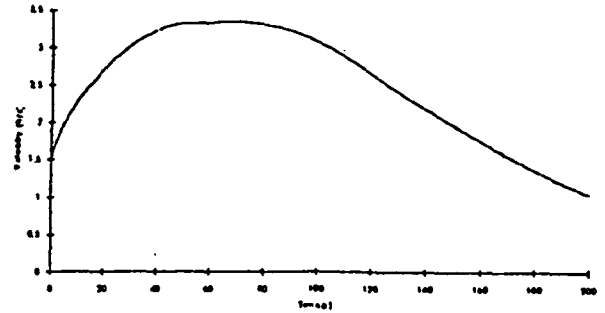


Figure 9. Rollout velocity profile.

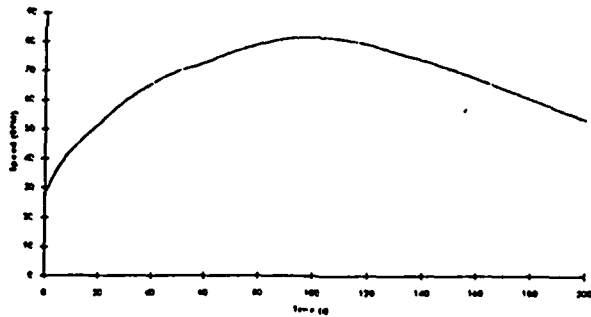


Figure 6. Rotational speed during reeldown.

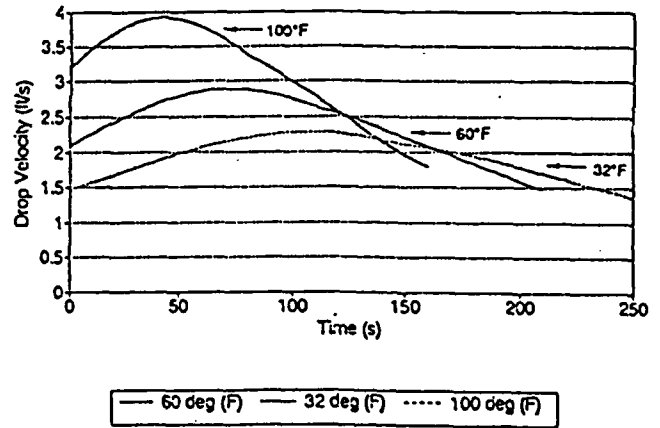


Figure 10. The effect of various starting temperatures on reeldown velocity.

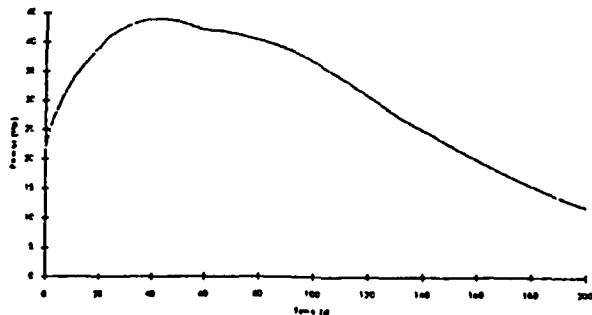


Figure 7. Brake Power during reeldown.